Journal of Visualized Experiments

Isolation of Primary Cancer-associated Fibroblasts from a Syngeneic Murine Breast Cancer for the Study of Targeted Nanoparticles
--Manuscript Draft--

Article Type:	Invited Methods Collection - JoVE Produced Video
Manuscript Number:	JoVE62504R1
Full Title:	Isolation of Primary Cancer-associated Fibroblasts from a Syngeneic Murine Breast Cancer for the Study of Targeted Nanoparticles
Corresponding Author:	Serena Mazzucchelli, Ph.D. University of Milan Milan, Milan ITALY
Corresponding Author's Institution:	University of Milan
Corresponding Author E-Mail:	serena.mazzucchelli@unimi.it
Order of Authors:	Marta Truffi
	Leopoldo Sitia
	Marta Sevieri
	Arianna Bonizzi
	Maria Antonietta Rizzuto
	Serena Mazzucchelli, Ph.D.
	Fabio Corsi
Additional Information:	
Question	**Response**
Please indicate whether this article will be Standard Access or Open Access.	Open Access (US$4,200)
Please specify the section of the submitted manuscript.	Cancer Research
Please indicate the **city, state/province, and country** where this article will be **filmed**. Please do not use abbreviations.	Milan, Milan, Italy
Please confirm that you have read and agree to the terms and conditions of the author license agreement that applies below:	I agree to the Author License Agreement
Please provide any comments to the journal here.	
Please indicate whether this article will be Standard Access or Open Access.	Open Access ($3900)

1   **TITLE:**
2   Isolation of Primary Cancer-associated Fibroblasts from a Syngeneic Murine Breast Cancer for the
3   Study of Targeted Nanoparticles
4
5   **AUTHORS AND AFFILIATIONS:**
6   Marta Truffi[1*], Leopoldo Sitia[2*], Marta Sevieri[2], Arianna Bonizzi[2], Maria Antonietta Rizzuto[3],
7   Serena Mazzucchelli[2], Fabio Corsi[1,2]
8
9   [1]Istituti Clinici Scientifici Maugeri IRCCS, Pavia, Italy
10   [2]Dipartimento di Scienze Biomediche e Cliniche "L. Sacco", Università di Milano, Milan, Italy
11   [3]Dipartimento di Biotecnologie e Bioscienze, Università di Milano-Bicocca, Milan, Italy
12
13   * These authors equally contributed to this work.
14
15   **Email addresses of co-authors:**
16   Marta Truffi   (marta.truffi@icsmaugeri.it)
17   Leopoldo Sitia   (leopoldo.sitia@unimi.it)
18   Marta Sevieri   (marta.sevieri@unimi.it)
19   Arianna Bonizzi   (arianna.bonizzi@unimi.it)
20   Maria Antonietta Rizzuto   (maria.rizzuto@unimib.it)
21
22   **Corresponding authors:**
23   Fabio Corsi   (fabio.corsi@unimi.it)
24   Serena Mazzucchelli   (serena.mazzucchelli@unimi.it)
25

26   **KEYWORDS:**
27   Cancer-associated fibroblast, *ex vivo* model, breast cancer, ferritin nanoparticles, active
28   targeting, 4T1-luc
29
30   **SUMMARY:**
31   This paper aims to provide a protocol for the isolation and culture of primary cancer-associated
32   fibroblasts from a syngeneic murine model of triple-negative breast cancer and their application
33   for the preclinical study of novel nanoparticles designed to target the tumor microenvironment.
34
35   **ABSTRACT:**
36   Cancer-associated fibroblasts (CAFs) are key actors in the context of the tumor
37   microenvironment. Despite being reduced in number as compared to tumor cells, CAFs regulate
38   tumor progression and provide protection from antitumor immunity. Emerging anticancer
39   strategies aim to remodel the tumor microenvironment through the ablation of pro-tumorigenic
40   CAFs or reprogramming of CAF functions and their activation status. A promising approach is the
41   development of nanosized delivery agents able to target CAFs, thus allowing the specific delivery
42   of drugs and active molecules. In this context, a cellular model of CAFs may provide a useful tool
43   for *in vitro* screening and preliminary investigation of such nanoformulations.

44 This study describes the isolation and culture of primary CAFs from the syngeneic 4T1 murine
45 model of triple-negative breast cancer. Magnetic beads were used in a 2-step separation process
46 to extract CAFs from dissociated tumors. Immunophenotyping control was performed using flow
47 cytometry after each passage to verify the process yield. Isolated CAFs can be employed to study
48 the targeting capability of different nanoformulations designed to tackle the tumor
49 microenvironment. Fluorescently labeled H-ferritin nanocages were used as candidate
50 nanoparticles to set up the method. Nanoparticles, either bare or conjugated with a targeting
51 ligand, were analyzed for their binding to CAFs. The results suggest that *ex vivo* extraction of
52 breast CAFs may be a useful system to test and validate nanoparticles for the specific targeting
53 of tumorigenic CAFs.
54
55 **INTRODUCTION:**
56 During the past decades, it has become clear that killing tumor cells is usually not sufficient to
57 eradicate malignancy, as the tumor microenvironment may prompt tumor relapse and induce
58 therapeutic resistance[1,2]. A novel paradigm has then emerged: targeting tumor stroma to deprive
59 the tumor of supporting factors and thus, boost the efficacy of chemotherapeutics[3–5]. In
60 particular, cancer-associated fibroblasts (CAFs) are an interesting stromal target in many solid
61 tumors[6,7]. CAFs are a very heterogeneous group of cells that interact with cancer cells and cells
62 of the immune system through the secretion of growth factors, cytokines, and chemokines; build
63 up and remodel the extracellular matrix; and enable metastasis formation[8–12]. Depending on the
64 tumor type, CAFs show pro-tumorigenic functions, while other subtypes of CAFs seem to have
65 tumor-suppressive functions[13,14]. To better clarify this dichotomy, a thorough characterization of
66 CAFs from primary and metastatic tumors is important.
67
68 In this context, an emerging field of research has focused on the development of nanosized
69 agents designed to target and/or destroy CAFs by delivering active molecules and drugs able to
70 remodel the tumor microenvironment[15–18]. Several types of nanoparticles have been designed to
71 achieve CAF ablation by cytotoxic drugs, to induce CAF-targeted photodynamic therapy, or to
72 reprogram CAFs by reverting them to a quiescent state or inducing TNF-related apoptosis
73 induced ligand expression, which induces apoptosis of neighboring cancer cells[16,19]. Moreover,
74 the potential of many nanoparticles to actively target specific biological markers gives rise to the
75 hope of selecting CAF subsets to target. Although its absolute specificity for CAF is still
76 questioned, fibroblast activation protein (FAP) is one of the most promising targets of pro-
77 tumorigenic stroma and is exploited to steer nanodrug delivery, thus paving the path for the
78 development of CAF-targeting nanotherapeutics[20–22].
79
80 This paper describes the isolation of primary CAFs from a syngeneic model of murine breast
81 cancer and reports their use in the study of the targeting capability of nanoparticles engineered
82 to recognize the CAF marker, FAP. Ferritin nanocages are used as candidate nanosystems to set
83 up the method, as their specificity of delivery may be shaped by the surface exposure of targeting
84 moieties[23,24]. Moreover, ferritins have been successfully proven to be excellent biocompatible
85 shuttles for antitumor applications, triggering rapid accumulation of the payload in the tumor
86 mass[25–27]. To date, preclinical studies of CAF-targeting nanosystems have involved *in vitro* testing
87 on fibroblast cell lines stimulated in culture with transforming growth factor-beta to induce cell

88   activation and the expression of some immunophenotypic features of CAFs[28,29]. This method is
89   usually applied to immortalized cell lines (such as NIH3T3, LX-2) and is quite rapid and simple,
90   yielding activated cells in a few hours or days. A limitation is that although *in vitro* stimulation
91   induces the expression of some genes attributed to activated myofibroblasts, it cannot entirely
92   recapitulate all the biological features of real CAFs, especially their heterogeneity *in vivo*.

93

94   Another strategy involves the extraction of primary CAFs from human or mouse tumor
95   samples[30,31]. This ensures that CAF activation occurs in a physiological context, and that the
96   heterogeneity of CAF subpopulations is maintained. According to the research objective, CAFs
97   may be derived from different sources, thus offering the possibility to study the most reliable
98   condition. The protocol reported here would be valuable for scientists who seek to perform a
99   preliminary evaluation of the functionality of novel nanoparticles designed to target CAFs from a
100   murine breast cancer model. Isolated CAFs would be useful for screening those nanoparticles
101   that are promising enough to proceed for *in vivo* evaluation in animal models of cancer. This will
102   be relevant during the first steps of nanoparticle production, driving nanotechnologists toward
103   the refinement of nanoparticle design by mainly considering the strategy of ligand immobilization
104   to achieve optimal targeting properties.

105

106   **PROTOCOL:**

107

108   **1.   Establishing a syngeneic 4T1 model of breast cancer**

109

110   NOTE: The present protocol describes the isolation of primary CAFs from a mouse 4T1 breast
111   tumor. The animal study described here has been approved by the Italian Ministry of Health (aut.
112   number 110/2018-PR).

113

114   1.1.   Tumor cell culture and implantation

115

116   1.1.1. Thaw 1×10^6 4T1-luc cells in a T75 flask with 10 mL of Roswell Park Memorial Institute
117   (RPMI) 1640 medium supplemented with 10% fetal bovine serum (FBS), 1%
118   penicillin/streptomycin (P/S), and 1% L-glutamine. Add Mycoplasma removal agent (1:100) in the
119   culture medium.

120

121   NOTE: 4T1-luc cells stably express luciferase and can be visualized by bioluminescence (BLI) upon
122   proper stimulation with D-luciferin. This allows *in vivo* monitoring of the viability and proliferation
123   of tumor cells upon implantation in mice (**Figure 1**).

124

125   1.1.2. Maintain the cells at 37 °C and 5% CO_2 in a humidified atmosphere until ~80% confluence,
126   by changing the medium every 2 days.

127

128   NOTE: Continue treatment with Mycoplasma removal agent for 1 week (~2/3 passages) before
129   injection in mice to ensure that injected cells are mycoplasma-free.

130

Page 3

131 1.1.3. On the day of the procedure, detach cells using 1 mL of trypsin-
132 ethylenediaminetetraacetic acid (EDTA) solution (trypsin 1:250) for 5 min at 37 °C. Stop trypsin
133 activity by adding culture medium, count the cells with trypan blue (1:1), and calculate the
134 number of cells/mL.

135

136 1.1.4. Pipette the volume corresponding to 1×10^6 cells and centrifuge for 5 min at $400 \times g$. Pour
137 off the supernatant, and resuspend the pellet in 1 mL of RPMI 1640 base medium. Keep the cells
138 on ice until ready for injection.

139

140 NOTE: For each mouse, 1×10^5 cells are needed; however, always calculate for an excess of 2
141 mice (corresponding to 2×10^5 cells) to ease syringe loading.

142

143 1.1.5. One day before the operation, shave the fur of 8 BALB/c mice (female, seven-week-old)
144 to expose the area of the abdominal mammary glands on the right side. Use an electric shaver
145 and apply a thin layer of depilatory cream for 4 min; then, wash away the cream with water and
146 a piece of paper.

147

148 1.1.6. Induce anesthesia by continuous inhalation of 2% isoflurane gas for ~5 min, and perform
149 a subcutaneous injection in the region of the abdominal mammary glands with a 27 G tuberculin
150 syringe. Turn the needle upwards to enter the skin subcutaneously; then, hold the skin upwards
151 and slowly inject 100 μL of cell suspension (1×10^5 cells). Slightly turn the needle around before
152 slowly retracting the syringe.

153

154 NOTE: Remember to bring the cell suspension to room temperature 15 min before injection.

155

156 1.2.   Tumor growth and dissection

157

158 1.2.1. At 5 days post-cell-injection, inject 150 mg/kg D-luciferin intraperitoneally (100 μL) 5 min
159 before imaging. Capture BLI images using an *in vivo* imaging system setting 10 s exposure,
160 medium binning, and f/stop at 4. Define the luminescent area of the tumor as the region of
161 interest (ROI), and quantify the total signal in the ROI (photon/sec/m^2) using imaging software.

162

163 1.2.2. Repeat the procedure of imaging (1.2.1) every 5 days from the injection to monitor tumor
164 growth in terms of an increase in BLI.

165

166 1.2.3. To establish the tumor volume, hold the mouse and expose its belly. Use calipers to
167 measure the tumor length (L) and width (W) once a week. Calculate the tumor volume (V) using
168 equation 1.

169

170 $[V = (L \times W^2)/2]$ (1)

171

172 1.2.4. At 20 days post-cell-injection, sacrifice the animals by cervical dislocation, dissociate the
173 tumors from the skin with scissors, and collect them in a tissue storage solution (see the **Table of**
174 **Materials**).

Page 4

175
176   NOTE: Tumor samples may be used immediately for section 2 or stored at 4 °C for up to 48 h.

177
178   2.   **Tumor dissociation into single cells**

179
180   NOTE: For the following steps, use sterile reagents and disposables in a laminar flow hood. Work
181   with 4 tumors per day.

182
183   2.1.   Place the tumor sample in a Petri dish, and carefully remove any fragment of skin, fat, and
184   necrotic areas with the help of tweezers and scalpel. Then, reduce the tumor into small pieces of
185   approximately 1–2 mm and transfer them to a tube (**Figure 2A**).

186
187   NOTE: 4T1 tumors become highly necrotic while growing, with a tendency to ulceration. It is
188   important to carefully remove the necrotic areas to avoid any interference of debris with the next
189   steps.

190
191   2.2.   Prepare a digestion mix for tumor dissociation: mix 2.35 mL of RPMI 1640 medium, 100
192   µL of enzyme D, 50 µL of enzyme R, and 12.5 µL of enzyme A. Soak the tumor fragments in the
193   solution and tightly close the tube.

194
195   NOTE: The indicated volumes of digestion mix are valid for tumors up to 1 g and may be adjusted
196   for larger tumors according to their weight. 4T1 tumors grown for 21 days normally are in a range
197   of 0.5–0.8 g.

198
199   2.3.   Turn the tube upside down, checking that all the pieces of tumor stand in the bottom of
200   the tube toward the cap. Attach the tube to a mechanical dissociator in the proper housing, and
201   run a specific dissociation program designed for tough tumors (see the manufacturer's
202   instructions).

203
204   NOTE: Special tubes may be required to fit into the dissociator. C-tubes bear a rotor inside the
205   cap to promote mechanical dissociation of the tissue.

206
207   2.4.   Detach the tube, maintain it upside down, and incubate the sample at 37 °C for 40 min
208   with gentle shaking. Then, attach the tube to the dissociator in the proper housing, and run the
209   following specific dissociation program designed for tough tumors two times. Ensure there are
210   no large pieces of tissue at the end of the procedure (**Figure 2B**).

211
212   NOTE: To dissociate the tumor, other enzyme cocktails could be used to degrade the extracellular
213   matrix. However, in this protocol, a commercially available Tumor Dissociation kit containing an
214   optimized enzyme mix (enzymes D, R, A) and a semi-automated dissociator that mechanically
215   dissociates the tissue were used. This combination ensured a proper degradation of the
216   extracellular matrix together with maintenance of cell integrity and cell surface epitopes.

217

218   2.5.   Filter the sample through a 40 μm cell strainer in a 50 mL tube, wash the filter with 10 mL
219   of RPMI 1640 medium, and centrifuge the tube for 7 min at 300 × g. If the cell pellet appears red,
220   lyse erythrocytes by adding 1 mL of Ammonium-Chloride-Potassium (ACK) lysing buffer for 5 min
221   at room temperature, wash with 10 mL of RPMI 1640, transfer the cell suspension in a 15 mL
222   tube, and centrifuge again.

223

224   2.6.   Resuspend the pellet in 1 mL of PBE buffer composed of phosphate-buffered saline (PBS),
225   0.5% bovine serum albumin (BSA), and 2 mM EDTA, and count the cells with trypan blue (1:1). In
226   case of cell clumps, filter the cell suspension through a 70 μm cell strainer, previously soaked
227   with PBS.

228

229   NOTE: Especially when tumors are big, it is important to check the cell count and eventually to
230   split each tumor sample in different tubes with no more than 10^7 cells in each tube before
231   proceeding to step 2.7.

232

233   2.7.   Prepare the dead cell removal binding buffer by diluting the 20x binding buffer stock
234   solution (see the **Table of Materials**) with sterile double-distilled water. Wash cells with 5 mL of
235   1× binding buffer (**Figure 2C**).

236

237   NOTE: Keep the buffer at 4 °C.

238

239   2.8.   Centrifuge for 7 min at 300 × g, and resuspend the cell pellet with 0.1 mL of dead cell
240   removal microbeads (see the **Table of Materials**). Mix well and incubate at room temperature
241   for 15 min.

242

243   2.9.   During the incubation with beads, prepare a magnetic stand under the hood and hang
244   ferromagnetic separation columns (one column for up to 10^7 cells) on it with the tips pointing
245   down. Equilibrate the columns with 0.5 mL of cold 1× binding buffer. Wait until the solution has
246   flowed through under gravity.

247

248   NOTE: It is important to not exceed the number of cells per column to avoid any risk of clotting
249   the column bed and reducing the recovery yield. When working with more than 10^7 cells, either
250   use more columns according to the total number of cells or use bigger columns. In such cases,
251   adjust the reagent volumes described in the following steps to the ones indicated by the
252   manufacturer.

253

254   2.10.   At the end of incubation, add 400 μL of cold 1× binding buffer to the bead/cell
255   suspension, load the entire volume onto the column, and collect the effluent (corresponding to
256   unlabeled cells) in a 15 mL tube.

257

258   2.11.   Wash the column four times with 0.5 mL of cold 1× binding buffer, and collect the total
259   effluent (corresponding to the live cell fraction) in the same tube.

260

261 2.12.   Count the cells with trypan blue (1:1). Place 1×10^5 cells in two tubes for Fluorescence
262 Activated Cell Sorting (FACS), and keep them at 4 °C until process validation (see step 4.1): use
263 the first tube to set the analysis parameters and the regions of positivity (control tube) and the
264 other one for biomarker analysis (sample tube). Use the remaining cells for CAF extraction (see
265 section 3).

266

267 NOTE: Removal of dead cells is important to reduce non-specific reactions with the microbeads
268 in section 3. However, to improve the yield, avoid the removal of dead cells if the proportion of
269 dead cells is <20%.

270

271 3.   **Extraction of primary CAFs from breast tumor**

272

273 NOTE: For section 3, use the mouse Tumor-Associated Fibroblast Isolation kit containing Non-
274 Tumor-Associated Fibroblast Depletion Cocktail and Tumor-Associated Fibroblast Microbeads
275 suited for magnetic labeling of the cells (see the **Table of Materials**).

276

277 3.1.   Depletion of non-cancer-associated fibroblasts

278

279 3.1.1. Moisten a 70 µm cell strainer with PBS, and filter the cell suspension to remove any
280 clumps. Then, centrifuge the cells for 10 min at 300 × g and aspirate the supernatant.

281

282 NOTE: If a single tumor was divided into two samples for step 2.7, pool the cell suspension two
283 by two before proceeding with step 3.1.2.

284

285 3.1.2. Resuspend the pellet in 80 µL of cold PBE buffer, and add 20 µL of Non-Tumor-Associated
286 Fibroblast Depletion Cocktail. Mix well and incubate at 4 °C for 15 min in the dark.

287

288 3.1.3. During the incubation with beads, prepare ferromagnetic depletion columns (1 per
289 sample) on a magnetic stand, and equilibrate the columns with 2 mL of cold PBE buffer. Wait
290 until the solution has flowed through.

291

292 3.1.4. At the end of incubation, add 400 µL of cold PBE buffer to the bead/cell suspension, load
293 the entire volume onto the column, and collect the effluent (corresponding to unlabeled cells) in
294 a 15 mL tube.

295

296 3.1.5. Wash the column twice with 2 mL of cold PBE buffer, and collect the total effluent in the
297 same tube. Centrifuge for 10 min at 300 × g and resuspend in 0.1 mL of cold PBE buffer.

298

299 NOTE: Depletion of non-cancer-associated fibroblasts drastically reduces the total amount of
300 cells recovered. It is generally necessary and recommended to pool cell suspensions from four
301 different samples to obtain a visible pellet and enough cells for step 3.2. This will ensure an
302 optimal yield.

303

304   3.1.6.   Place 20 mL of the cell suspension in a FACS tube and keep it at 4 °C for process validation
305   (see section 4). Use the remaining cells for CAF selection (see step 3.2).
306
307   3.2.   Positive selection of cancer-associated fibroblasts
308
309   3.2.1.   Add 20 µL of Tumor-Associated Fibroblast Microbeads to 80 µL of cell suspension. Mix
310   well and incubate at 4 °C for 15 min in the dark.
311
312   3.2.2.   During incubation with beads, prepare ferromagnetic separation columns (1 per sample)
313   on a magnetic stand, and equilibrate the columns with 0.5 mL of cold PBE buffer. Wait until the
314   solution has flowed through.
315
316   3.2.3.   At the end of the incubation, add 400 µL of cold PBE buffer to the bead/cell suspension,
317   load the entire volume onto the column, and let the unlabeled cells flow through into a 15 mL
318   tube.
319
320   3.2.4.   Wash the column three times with 0.5 mL of cold PBE buffer, and collect the total effluent
321   in the same tube.
322
323   NOTE: The flow-through contains unlabeled CD90.2-negative cells, which may be discarded as
324   non-cancer-associated fibroblasts.
325
326   3.2.5.   Remove the column from the magnet and place it in a 1.5 mL tube. Add 1 mL of cold PBE
327   onto the column, and immediately push the plunger into the column to flush the cells out.
328
329   3.2.6.   Centrifuge for 10 min at 400 × g and resuspend in 0.1 mL of cold PBE buffer. Place 20 µL
330   of cell suspension in a FACS tube and keep it at 4 °C for process validation (see section 4).
331
332   NOTE: After centrifuging, the pellet may be hardly visible, especially when the original tumors
333   are small. Use conical bottom centrifuge tubes and be careful not to lose any cells when aspirating
334   the supernatant.
335
336   3.2.7.   Dilute the remaining cells in an appropriate volume of Dulbecco's Modified Eagle's
337   Medium (DMEM)/Ham's F-12 supplemented with 15% FBS, 2 mM L-glutamine, 1% P/S, and 1%
338   non-essential amino acids, and seed the cells in a tissue-culture plate.
339
340   3.2.8.   Check the cell density under a microscope, and place the plate in an incubator at 37 °C
341   and 5% CO_2 to let the cells adhere and grow.
342
343   NOTE: If the cells are too dense, immediately split the cell suspension into two wells of the tissue
344   culture plate before placing the plate in the incubator.
345
346   **4.   Process validation**
347

348   4.1.   Flow cytometry

349

350   NOTE: Section 4.1 does not require sterile conditions and can be performed outside the laminar
351   hood. Perform section 4.1 in parallel for samples collected in step 2.11 (dissociated tumor), step
352   3.1.6 (after depletion of non-cancer-associated fibroblasts), and step 3.2.6 (after enrichment of
353   cancer-associated fibroblasts).

354

355   4.1.1.   Centrifuge the FACS tubes prepared in steps 2.11, 3.1.6, and 3.2.6 for 10 min at 300 × g.
356   Discard the supernatant.

357

358   NOTE: Prepare at least one additional tube, which contains unstained cells acting as a control to
359   set the parameters for analysis.

360

361   4.1.2.   In sample tubes, resuspend cells in 88 μL of PBE, and add 2 μL of anti-CD45 antibody
362   conjugated with fluorescein isothiocyanate (FITC, 1:50 dilution, according to the manufacturer's
363   instructions) and 10 μL of anti-CD90.2 antibody conjugated with phycoerythrin (PE, 1:10 dilution,
364   according to the manufacturer's instructions). Mix thoroughly and incubate for 10 min at 4 °C in
365   the dark. In the control tube (unstained), resuspend cells in 100 μL of PBE. Incubate for 10 min at
366   4 °C in the dark to replicate the procedure followed for antibody-stained cells.

367

368   NOTE: Temperature and time of incubation must be checked carefully, as a variation in such
369   variables might result in poor or non-specific staining, thus altering the results.

370

371   4.1.3.   After completing the incubation step, perform a wash by adding 1 mL of PBE. Centrifuge
372   for 10 min at 300 x g. Discard the supernatant.

373

374   4.1.4.   Resuspend cells (all tubes) in 500 μL of PBS.

375

376   4.1.5.   Mix well and proceed with flow cytometry analysis. Set the channels to measure the
377   fluorescence of the antibodies (i.e., FITC and PE).

378

379   4.1.6.   From the control tube, select all viable cells by drawing a first gate (P1) on the Forward
380   versus Side scatter (FSC vs SSC) plot. Within P1, set a second gate (P2) comprising single cells
381   only.

382

383   4.1.7.   Using the specific fluorescence channels of the antibodies (i.e., FITC and PE), set proper
384   gates to discern positively stained cells.

385

386   4.1.8.   Start the analysis and record at least 10,000 events in P2. Read signals from both channels
387   simultaneously.

388

389   NOTE: If the overall number of cells is less than expected, it could be preferable to read the whole
390   tube.

391

392 4.1.9. (OPTIONAL) If further staining with additional antibodies/fluorophores is programmed,
393 set an appropriate compensation matrix before initiating the analysis.
394
395 4.2.   Monitoring of cell morphology and characteristics
396
397 NOTE: Once seeded, the cells must be handled under sterile conditions.
398
399 4.2.1. On the day after seeding, visualize the cells under an optical microscope to check cell
400 adhesion and morphology. Aspirate the supernatant and replace with fresh medium.
401
402 NOTE: CAFs are large spindle-shaped cells, which can be easily distinguished from the epithelial-
403 like structure of 4T1 tumor cells.
404
405 4.2.2. Maintain the cells at 37 °C and 5% CO_2 in a humidified atmosphere, changing the medium
406 every 2 days.
407
408 4.2.3. When cells reach ~80% confluence (approximately 4-6 days after seeding), detach the
409 cells using TrypLE Select solution (see the **Table of Materials**) for 5 min at room temperature.
410 Add fresh medium (4:1), centrifuge the cell suspension at 400 × g for 5 min, and resuspend the
411 pellet in fresh medium.
412
413 4.2.4. Split the cells 1:2, and expand the culture until the number of cells needed for the
414 experiment is obtained.
415
416 4.2.5. At each passage, check cell morphology and growth under an optical microscope. If cell
417 morphology is not homogeneous (e.g., clones of small round-shape cells appearing in culture),
418 analyze a sample of cells by flow cytometry as described in section 4.1. If homogeneous, proceed
419 to step 4.2.7.
420
421 NOTE: Changes in cell morphology may indicate contamination by non-cancer-associated
422 fibroblasts, which need to be removed to ensure culture purity.
423
424 4.2.6. Analyze the flow cytometry results and proceed according to one of the following
425 scenarios: (i) if contamination of CD90.2-/CD45- cells occurs, collect all the cells, and repeat the
426 positive selection by following step 3.2; (ii) if contamination of CD45+ cells also occurs, collect all
427 the cells, and repeat the depletion in step 3.1; (iii) if no contamination occurs (only
428 CD90.2+/CD45- cells are present), keep the cells in culture and proceed directly to 4.2.7.
429
430 NOTE: As repeating the depletion process with microbeads will reduce cell recovery, it is
431 recommended only when cells do not need to be used immediately.
432
433 4.2.7. Count the cells with trypan blue (1:1), place 5 × 10^5 cells in two FACS tubes, and centrifuge
434 for 10 min at 300 × g. Discard the supernatant, and resuspend the pellet in 0.5 mL of blocking
435 buffer (PBS supplemented with 2% BSA, 2% goat serum) for 15 min at room temperature.

436

437 NOTE: One tube acts as a control consisting of unstained cells only, while cells in the second tube
438 will be stained for flow cytometry analysis.

439

440 4.2.8. Centrifuge for 10 min at 300 × g, discard the supernatant and resuspend in 99 µL of
441 blocking buffer. Add 1 µg of anti-FAP antibody to the sample tube and 1 mL of blocking buffer to
442 the control tube. Mix thoroughly and incubate for 15 min at room temperature.

443

444 NOTE: FAP is a surface marker of reactive tumor stroma and may be used to identify and
445 characterize CAFs.

446

447 4.2.9. Wash thrice with PBS, centrifuge, and incubate with the appropriate secondary antibody
448 conjugated with a fluorescent dye (1 µg) in blocking buffer for 15 min at room temperature.

449

450 4.2.10. Wash thrice with PBS, and analyze by flow cytometry (follow steps 4.1.5 to 4.1.7 by setting
451 the appropriate channel to detect the fluorophore used). Then, use the cells for experiments
452 (step 5.2).

453

454 4.2.11. (OPTIONAL) Freeze a sample of cells in 1 mL of 90% FBS and 10% dimethyl sulfoxide
455 (DMSO); store at -80 °C for further use.

456

457 5. **CAF targeting by engineered Ferritin nanoparticles**

458

459 NOTE: A recombinant variant of human ferritin heavy chain (HFn) was used as bare nanoparticle
460 or was conjugated with targeting moieties. Here, HFn nanoparticles functionalized with the
461 variable portion of an anti-FAP antibody (Fab@FAP) were prepared by the NanoBioLab at
462 University of Milano-Bicocca at two HFn:Fab@FAP molar ratios, 1:1 and 1:5, according to a
463 previously described protocol[32].

464

465 5.1. Fluorescent labeling of Ferritin nanoparticles

466

467 NOTE: Both bare and functionalized HFn nanocages are fluorescently labelled with FITC.

468

469 5.1.1. Dissolve the FITC powder in 99% ethanol to obtain a concentration of 2 mg/mL.

470

471 NOTE: This solution should be prepared freshly.

472

473 5.1.2. Incubate 50 µL of the prepared solution (200 µg of FITC) for every 1 mg of protein (i.e.,
474 100 µL of HFn at 10 mg/mL). Add 50 µL of 1 M sodium bicarbonate ($NaHCO_3$), and adjust the
475 volume to 500 µL with 0.1 M $NaHCO_3$.

476

477 NOTE: Scale up the volumes according to the experimental needs.

478

479 5.1.3. Incubate the reaction mixture at room temperature, in the dark, and with continuously
480 stirring for 1 h.
481
482 5.1.4. Remove the excess of FITC from the conjugate by gel filtration using a spin desalting
483 column (7K MWCO).
484
485 5.1.5. Assess the concentration of the recovered labelled protein by using a spectrophotometer.
486 Estimate amounts of protein and dye by measuring the absorbance at 280 nm and at 488 nm,
487 respectively.
488
489 5.2. Binding of Ferritin nanoparticles to CAFs
490
491 NOTE: Use CAFs from no later than passages 4–5 in culture.
492
493 5.2.1. Place 5×10^5 cells in each FACS tube, centrifuge for 10 min at 300 × g, and resuspend in
494 0.5 mL of PBS, 0.3% BSA supplemented with 0.1 mg/mL of the different preparations of
495 nanoparticles (bare HFn, HFn-Fab@FAP 1:1, HFn-Fab@FAP 1:5) previously labeled with FITC.
496
497 NOTE: Run each condition in triplicate. Prepare an additional tube as a control unlabeled sample
498 to which no nanoparticles are added.
499
500 5.2.2. Incubate for 2 h at 4 °C in the dark, centrifuge, and wash three times in PBS.
501
502 5.2.3. Resuspend cells with 0.5 mL PBS, mix well, and analyze by flow cytometry. Set the
503 channels to measure the fluorescence of FITC.
504
505 5.2.4. After gating on live single cells, acquire 20,000 events. Use the control unlabeled tube to
506 set the gate of FITC positivity and obtain the percentage of FITC$^+$ events (corresponding to
507 nanoparticle binding).
508
509 **6. Statistical analysis and experimental replicates**
510
511 6.1. Animals
512
513 6.1.1. Perform three independent experiments of tumor growth and CAF isolation, using 8
514 animals per single experiment, as described in 1.1.5. To optimize CAF isolation yield, divide the
515 excised tissues into subgroups (n=4) and process them, following steps described in section 2.
516
517 6.2. HFn interaction with cells
518
519 6.2.1. Evaluate the interaction of functionalized and non-functionalized HFn with target and
520 non-target cells (CAFs and 4T1, respectively) in terms of the percentage of positively stained cells
521 by fluorescently labelled nanocages. Report the results as average ± standard deviation of three
522 independent experiments.

Page 12

523

524   6.3.   Statistical analysis

525

526   6.3.1.   To calculate statistical significance in cell binding experiments with HFn and HFn-FAP, use
527   the ordinary one-way ANOVA test.

528

529   **REPRESENTATIVE RESULTS:**

530

531   ***In vivo* model set-up for optimal CAF isolation**
532   The injection of 10^5 4T1-luc cells into the mammary fat pad of female BALB/c mice leads to the
533   growth of a detectable tumor mass at 5 days after implantation. By measuring the tumor volume
534   by calipers and the tumor cell viability by BLI, tumor growth was monitored for one month after
535   implantation. To find a sacrifice window that is adequate for CAF isolation, an optimal
536   compromise was sought between higher tumor size and BLI on the one hand and an emerging
537   tumor ulceration and necrosis on the other hand (**Figure 1**). As a necrotic core appears 20 days
538   after implantation, and it enlarges at 25 and 30 days (as documented by BLI images in **Figure 1C**),
539   day 20 was set as the time point to optimize cell recovery after the isolation process. Even after
540   carefully removing all visible necrotic areas during the first steps of tumor handling *ex vivo*, a high
541   percentage of dead cells was found at the end of dissociation into single cells (**Table 1**). As this
542   percentage may be relevant, especially with the increase in tumor size, dead cell removal is
543   always necessary when working with the 4T1 model.

544

545   **Optimization of CAF isolation procedure, culture, and characterization**
546   Two more passages are needed to isolate the population of CAFs (CD90.2$^+$ CD45$^-$) from the panel
547   of collected viable cells: the depletion of non-tumor-associated fibroblasts and the enrichment
548   of tumor-associated fibroblasts (**Figure 2**). The depletion bead cocktail efficiently removes CD45$^+$
549   cells (accounting for 67.35% and 0.69% of total cells pre- and post-depletion, respectively, **Table
550   2**), and was always used to process one single tumor in every column. As shown in **Table 1**, the
551   number of eluted cells dropped from an average of 3×10^6 to 1×10^5 after the depletion step.
552   Due to this massive decrease in total cell number, it is convenient to pool the collected cells from
553   at least 2 to a maximum of 4 tumors in a single tube before proceeding with the enrichment step.
554   By doing so, an adequate number of cells was obtained for incubation with tumor-associated
555   fibroblast beads and passed through a single separation column to obtain a final average of 93%
556   of CD90.2$^+$ CD45$^-$ cells (**Table 2**).

557

558   Once seeded onto tissue culture plates, these recovered cells attached to the plastic and revealed
559   a large spindle-shaped morphology typical of fibroblasts (**Figure 3A,B**) and different from 4T1
560   tumor cells (**Figure 3D**). Not pooling tumors after depletion causes the cellular yield with tumor-
561   associated fibroblast microbeads to be too low to establish a culture. In other cases, when the
562   duration and temperature of the incubations with microbeads are not carefully maintained, some
563   non-specific binding may occur. In such cases, the enrichment steps were less efficient and higher
564   percentages of CD90.2$^-$ CD45$^+$ and CD90.2$^-$ CD45$^-$ cells were recovered along with the CD90.2$^+$
565   CAFs (5.97 ± 1.5 and 16.75 ± 1.1, respectively) (**Figure 4** and **Table 3**). These contaminant cells
566   were likely to be responsible for the presence in culture of small clones with different

Page 13

morphology (**Figure 4B**, black arrowheads) that grew faster than CAFs and prevailed over the primary CAF culture (**Figure 4C**). These suboptimal results confirmed the importance of always double-checking both CD90.2 and CD45 expression, as well as cell morphology at the end of the enrichment process and during cell growth in culture.

Use of isolated cells to evaluate CAF-targeting potential of engineered nanodrugs
The freshly isolated CAFs can be used for several applications ranging from basic research to pharmacological studies. This group's aim is to develop HFn nanocages that can specifically target CAFs. HFn was functionalized with a specific anti-FAP antibody fragment (HFn-FAP) at two different protein:antibody ratios (a lower 1:1 and a higher 1:5), and their binding with CAFs was tested. As FAP was used as a surface biomarker of pro-tumorigenic CAFs, it was of fundamental importance to check FAP expression on isolated CAFs (**Figure 3C**). FAP expression was followed over 5 passages in culture to confirm that the primary CAF culture maintained its original characteristics.

FAP functionalization on HFn was found to contribute to a significant shift toward CAF targeting as compared to bare HFn, and the lower amount of antibody (1:1) was enough to observe this effect (**Figure 5A**). However, this was not observed with the tumor 4T1 cells used to set up the *in vivo* tumor model, wherein bare HFn showed higher binding than functionalized HFn (**Figure 5B**). This was most likely due to the absence of FAP overexpression in 4T1 cells and the preferential interaction of HFn with TfR1, which regulates HFn uptake in cells, as widely reported by this group[27,33]. These results confirm the usefulness of using primary cultures of breast CAFs to preliminarily screen the targeting capability of nanoparticles designed to tackle the tumor microenvironment.

FIGURE AND TABLE LEGENDS:
Figure 1: **Establishment of the 4T1 tumor model.** Cells (10^5 cells/mouse) were injected into the mammary fat pad. Tumor growth was followed at days 5, 10, 15, 20, 25, and 30 after implantation (**A**) by measuring tumor volume with calipers and (**B**) by bioluminescence imaging. Tumor volumes and BLI are expressed as mm^3 and counts, respectively. Results are reported as average ± SEM (n=6). (**C**) BLI representative images obtained 5, 10, 15, 20, 25, and 30 days after cell implantation confirm tumor growth until day 25, when it seems to reach a plateau. At the last time point of analysis (30 days), the BLI does not increase as compared to day 25. Starting at day 20, areas of necrosis and ulceration start to become visible in the central part of the tumor. Color Scale: Min = 1,194, Max = 20,462. Abbreviations: BLI = bioluminescence imaging; SEM = standard error of the mean.

Figure 2: **Tumor sample preparation and flow cytometry characterization of isolated CAFs.**
Tumors were excised and reduced into (**A**) small pieces of approximately 1–2 mm with the help of a scalpel; (**B**) single cell suspension after tissue digestion and mechanical dissociation of an excised tumor; (**C**) cell pellet obtained after lysis of red blood cells; (**D**) flow cytometry analysis of CD45 and CD90.2 expression in cells obtained after removal of red blood cells and dead cells, (**E**) after depletion of non-cancer-associated fibroblasts, and (**F**) after enrichment of cancer-associated fibroblasts, where the majority of cells are CD90.2$^+$ CD45$^-$ (blue rectangle).

Page 14

611 Abbreviations: CAFs= cancer-associated fibroblasts; CD = cluster of differentiation; PE-A = area of
612 phycoerythrin; FITC-A = areas of fluorescein isothiocyanate.
613
614 **Figure 3: Morphological analysis of CAFs and FAP expression. (A, B)** CAF morphology was
615 checked throughout all passages of culture by optical microscopy (different levels of confluence
616 at passage 2 and passage 5) and compared to (**D**) 4T1 tumor cells; scale bars = 10 μm. (**C**)
617 Fibroblast activation protein (FAP) expression was evaluated by flow cytometry at the end of the
618 isolation process on the collected CD90.2$^+$ CD45$^-$ cells to confirm their molecular characteristics.
619 A fluorescence threshold was set on unstained control cells (red graph) to quantify mean
620 fluorescence intensity and the percentage of positive cells (FAP$^+$) among antibody-stained cells
621 (blue graph). Abbreviations: CAFs= cancer-associated fibroblasts; FAP = fibroblast activation
622 protein; CD = cluster of differentiation; MFI = mean fluorescence intensity; Ab = antibody; FITC-
623 A = area of fluorescein isothiocyanate; FAP+ = FAP-positive cells.
624
625 **Figure 4**: **Example of a sub-optimal CAF isolation process.** (**A**) Flow cytometry evaluation after
626 the final isolation step revealed the presence of contaminant CD90.2$^-$ CD45$^+$ and CD90.2$^-$ CD45$^-$
627 cells. (**B**) These cells can be seen as clones with small round morphology upon seeding (black
628 arrowheads and inset in the bottom left corner of the panel) that (**C**) prevailed over CAFs after
629 the third passage in culture. Scale bars = 10 μm. Abbreviations: CAF = cancer-associated
630 fibroblast; CD = cluster of differentiation; PE-A = area of phycoerythrin; FITC-A = areas of
631 fluorescein isothiocyanate.
632
633 **Figure 5**: **Binding of HFn nanocages on CAFs and 4T1.** HFn nanocages were fluorescently labeled
634 with FITC, functionalized with an anti-FAP antibody fragment (HFn-FAP) at two different protein-
635 antibody ratios (1:1 and 1:5), and incubated with (**A**) target CAFs and (**B**) 4T1 cells at 4 °C for 2 h.
636 Binding was evaluated by flow cytometry. (**A**) HFn-FAP binding with CAFs is significantly increased
637 at both antibody fragment concentrations by three-fold as compared to bare HFn. (**B**) in contrast,
638 a significantly higher binding of bare HFn was observed in 4T1 cells, where binding is not
639 enhanced by FAP recognition. Results are reported as average ± standard deviation of three
640 independent experiments. *** p = 0.0003; °° p = 0.0021 ; °°° p = 0.0008. Abbreviations: CAFs=
641 cancer-associated fibroblasts; FAP = fibroblast activation protein; HFn = recombinant variant of
642 human ferritin heavy chain used as bare nanoparticle or conjugated; HFN-FAP = HFn
643 nanoparticles functionalized with the variable portion of an anti-FAP antibody prepared at two
644 HFn:Fab@FAP molar ratios, 1:1 and 1:5.
645
646 **Table 1: Total cell count after each step of isolation of cancer-associated fibroblasts.**
647
648 **Table 2: Cell distribution according to expression of CD90.2 and CD45 after each passage of**
649 **isolation of cancer-associated fibroblasts.**
650
651 **Table 3: CD90.2 and CD45 expression of cells collected after a sub-optimal cancer-associated**
652 **fibroblast isolation experiment.**
653
654 **DISCUSSION:**

CAFs are emerging as key players in remodeling extracellular matrix, promoting metastasis progression, and limiting drug access to the tumor site[34]. However, due to their heterogeneity, their roles are still controversial—some CAFs are tumorigenic, whereas some other subtypes seem to have a tumor-suppressive role. In this context, their isolation can be of extreme interest to shed more light on their much-debated role in cancer progression, which will have important clinical implications[12,31]. Moreover, successful CAF extraction from human and preclinical mouse tumor models would also facilitate the development of new CAF-targeting drugs. This paper reports a method to efficiently isolate and culture primary CAFs from a syngeneic preclinical model of breast cancer. Based on experience, three experimental steps mostly influence the success of the protocol.

The first one is working fast to avoid aggregation of cell suspensions associated with the risk of clotting in the column and slowing cell efflux: in fact, when cells that passed through the column were clustered together, the probability of a sub-optimal isolation process increased, and the final cultures contained "contaminant" cell clones. The second one is pooling cells from different tumors after the depletion passage to guarantee enough cells to be passed through in the final enrichment step. The final critical issue is plating the extracted cells at high cell densities, most likely starting from a single well of the 24-well plate to boost cell growth and colony expansion for up to 4–5 passages. If the cells were seeded at low densities, they expanded on the free surface and quickly stopped replicating.

Several studies have already described CAF extraction methods of both human and mouse origin, to study their role in promoting cancer development and invasiveness. This has been done in many types of tumors, including breast cancer, melanoma, cholangiocarcinoma, and pancreatic adenocarcinoma[35-38]. However, due to the lack of specific CAF markers and to their heterogeneity, the results of these processes are still sub-optimal.
Here, the isolated cells were used to validate the CAF-targeting ability of HFn nanocages functionalized with anti-FAP targeting moieties. The use of primary cultures of CAFs was a significant advantage, allowing the validation of the nanostrategy *ex vivo* with a much simpler and cost-effective binding experiment than doing it directly *in vivo* at this preliminary phase of nanodrug optimization.

In this sense, *ex vivo* testing on CAFs can precede *in vivo* animal experiments by allowing the screening and selection of the most promising nanoparticles for the optimal targeting of CAF. The CAF model presented here may also be used for preliminary efficacy studies, when loading nanoparticles with active drugs. Animals will be only used later to evaluate biodistribution, pharmacokinetics, and efficacy studies.
Several CAF-targeting nanodrugs are being developed, such as ferritin nanocages for photodynamic therapy in breast cancer and peptide-based particles to deliver doxorubicin in prostate cancer models[39,40]. However, not many studies have focused on the isolation of CAFs as cell platforms for nanodrug optimization.

This protocol has some limitations. First, it is a time-consuming protocol, requiring the preparation and purchase of several reagents and materials. Second, due to the scarcity of CAFs

Page 16

699 in the 4T1 breast tumor, their yield is low. Nanoparticle experiments should be planned and
700 performed as soon as the required cell number is achieved, as primary CAFs undergo senescence
701 and cannot be maintained in culture for a long time. In conclusion, this method of CAF isolation,
702 culturing, and characterization can be a powerful tool to accelerate the development of new
703 targeted nanomedicines in the fight against cancer.
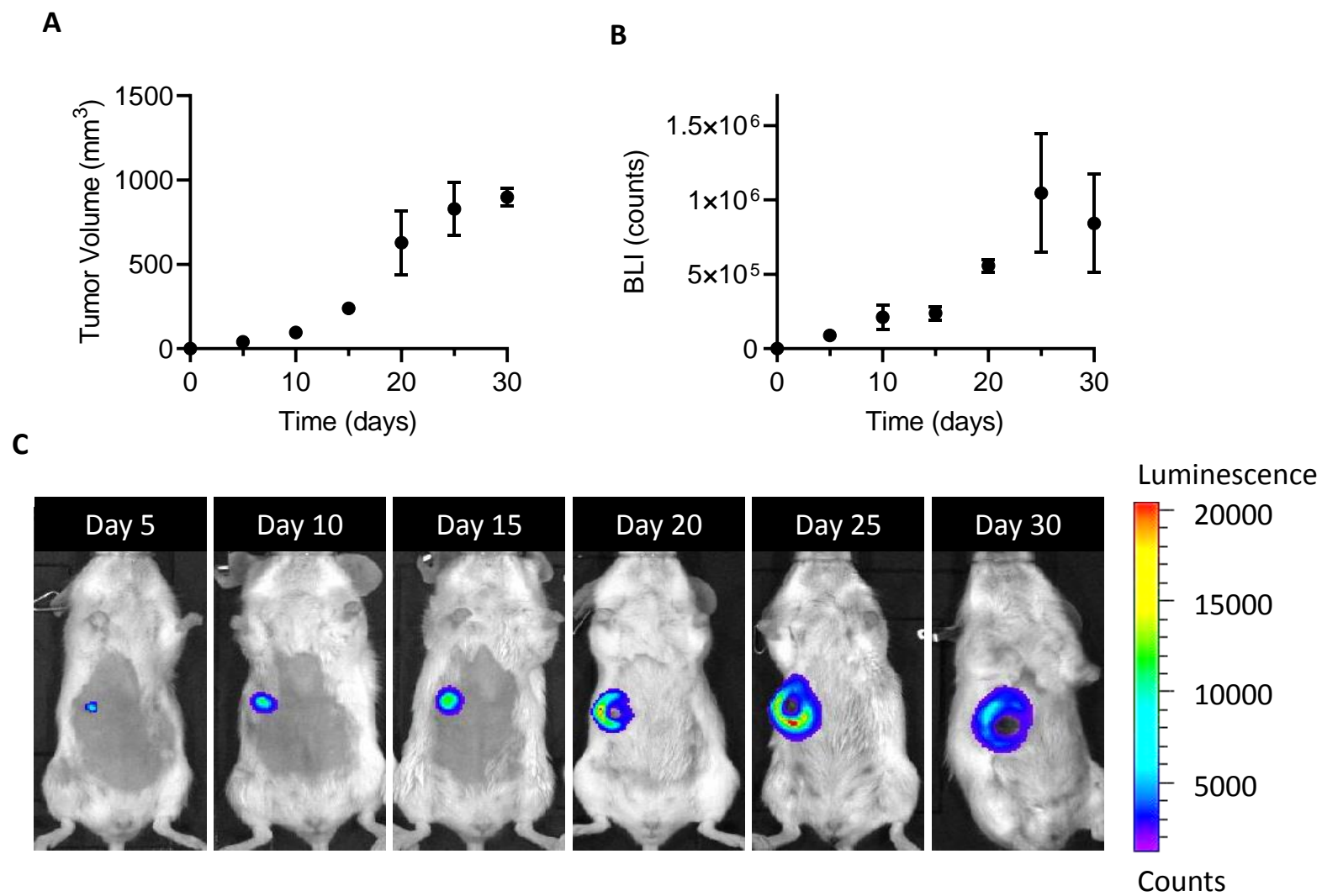704
712 **DISCLOSURES:**
713 The authors have nothing to disclose.
714

715 **REFERENCES:**
716 1.   Quail, D. F., Joyce, J. A. Microenvironmental regulation of tumor progression and
717 metastasis. *Nature Medicine.* **19** (11), 1423–1437 (2013).
718 2.   Velaei, K., Samadi, N., Barazvan, B., Soleimani Rad, J. Tumor microenvironment-mediated
719 chemoresistance in breast cancer. *Breast.* **30**, 92–100 (2016).
720 3.   Cheng, J. D., Weiner, L. M. Tumors and their microenvironments: tilling the soil.
721 Commentary re: A. M. Scott et al., A Phase I dose-escalation study of sibrotuzumab in patients
722 with advanced or metastatic fibroblast activation protein-positive cancer. Clin. Cancer Res., 9:
723 1639-1647, 2003. *Clinical Cancer Research.* **9** (5), 1590–1595 (2003).
724 4.   Hui, L., Chen, Y. Tumor microenvironment: Sanctuary of the devil. *Cancer Letters.* **368** (1),
725 7–13 (2015).
726 5.   Balkwill, F. R., Capasso, M., Hagemann, T. The tumor microenvironment at a glance.
727 *Journal of Cell Science.* **125**, 5591–5596 (2012).
728 6.   Chen, X., Song, E. Turning foes to friends: targeting cancer-associated fibroblasts. *Nature
729 Review. Drug Discovery.* **18** (2), 99–115 (2019).
730 7.   Franco, O. E., Shaw, A. K., Strand, D. W., Hayward, S. W. Cancer associated fibroblasts in
731 cancer pathogenesis. *Seminars in Cell & Developmental Biology.* **21** (1), 33–39 (2010).
732 8.   LeBleu, V. S., Kalluri, R. A peek into cancer-associated fibroblasts: origins, functions and
733 translational impact. *Disease Models & Mechanisms.* **11**, dmm029448 (2018).
734 9.   Li, X.-Y., Hu, S.-Q., Xiao, L. The cancer-associated fibroblasts and drug resistance. *European
735 Review for Medical and Pharmacological Sciences.* **19** (11), 2112–2119 (2015).
736 10.   Luo, H., Tu, G., Liu, Z., Liu, M. Cancer-associated fibroblasts: a multifaceted driver of breast
737 cancer progression. *Cancer Letters.* **361** (2), 155–163 (2015).
738 11.   Truffi, M., Sorrentino, L., Corsi, F. Fibroblasts in the tumor microenvironment. *Advances
739 in Experimental Medicine and Biology.* **1234**, 15–29 (2020).
740 12.   Sugimoto, H., Mundel, T. M., Kieran, M. W., Kalluri, R. Identification of fibroblast
741 heterogeneity in the tumor microenvironment. *Cancer Biology & Therapy.* **5** (12), 1640–1646
742 (2006).

Page 17

743   13.   Costa, A. et al. Fibroblast heterogeneity and immunosuppressive environment in human
744   breast cancer. *Cancer Cell.* **33** (3), 463–479.e10 (2018).
745   14.   Ishii, G., Ochiai, A., Neri, S. Phenotypic and functional heterogeneity of cancer-associated
746   fibroblast within the tumor microenvironment. *Advances Drug Delivery Reviews.* **99** (Part B), 186–
747   196 (2016).
748   15.   Chen, Q. et al. Remodeling the tumor microenvironment with emerging
749   nanotherapeutics. *Trends in Pharmacological Sciences.* **39** (1), 59–74 (2018).
750   16.   Truffi, M. et al. Nano-strategies to target breast cancer-associated fibroblasts: rearranging
751   the tumor microenvironment to achieve antitumor efficacy. *International Journal of Molecular*
752   *Sciences.* **20** (6), 1263 (2019).
753   17.   Tong, R., Langer, R. Nanomedicines Targeting the Tumor Microenvironment. *Cancer*
754   *Journal.* **21** (4), 314–321 (2015).
755   18.   Kaps, L., Schuppan, D. Targeting cancer associated fibroblasts in liver fibrosis and liver
756   cancer using nanocarriers. *Cells.* **9** (9), 2027 (2020).
757   19.   Miao, L. et al. Targeting tumor-associated fibroblasts for therapeutic delivery in
758   desmoplastic tumors. *Cancer Research.* **77** (3), 719–731 (2017).
759   20.   Kelly, T., Huang, Y., Simms, A. E., Mazur, A. Fibroblast activation protein-α: a key
760   modulator of the microenvironment in multiple pathologies. *International Review of Cell and*
761   *Molecular Biology.* **297**, 83–116 (2012).
762   21.   Brennen, W. N., Isaacs, J. T., Denmeade, S. R. Rationale behind targeting fibroblast
763   activation protein-expressing carcinoma-associated fibroblasts as a novel chemotherapeutic
764   strategy. *Molecular Cancer Therapeutics.* **11** (2), 257–266 (2012).
765   22.   Juillerat-Jeanneret, L., Tafelmeyer, P., Golshayan, D. Fibroblast activation protein-α in
766   fibrogenic disorders and cancer: more than a prolyl-specific peptidase? *Expert Opinion on*
767   *Therapeutic Targets.* **21**, 977–991 (2017).
768   23.   Falvo, E. et al. Antibody-drug conjugates: targeting melanoma with cisplatin encapsulated
769   in protein-cage nanoparticles based on human ferritin. *Nanoscale.* **5** (24), 12278–12285 (2013).
770   24.   Truffi, M. et al. Ferritin nanocages: A biological platform for drug delivery, imaging and
771   theranostics in cancer. *Pharmacological Research.* **107**, 57–65 (2016).
772   25.   Cai, Y. et al. Enhanced magnetic resonance imaging and staining of cancer cells using
773   ferrimagnetic H-ferritin nanoparticles with increasing core size. *International Journal of*
774   *Nanomedicine.* **10**, 2619–2634 (2015).
775   26.   Heger, Z., Skalickova, S., Zitka, O., Adam, V., Kizek, R. Apoferritin applications in
776   nanomedicine. *Nanomedicine.* **9** (14), 2233–2245 (2014).
777   27.   Mazzucchelli, S. et al. Nanometronomic treatment of 4T1 breast cancer with nanocaged
778   doxorubicin prevents drug resistance and circumvents cardiotoxicity. *Oncotarget.* **8** (5), 8383–
779   8396 (2017).
780   28.   Yu, Q. et al. Targeting cancer-associated fibroblasts by dual-responsive lipid-albumin
781   nanoparticles to enhance drug perfusion for pancreatic tumor therapy. *Journal of Controlled*
782   *Release.* **321**, 564–575 (2020).
783   29.   Mertens, J. C. et al. Therapeutic effects of deleting cancer-associated fibroblasts in
784   cholangiocarcinoma. *Cancer Research.* **73** (2), 897–907 (2013).
785   30.   Kovács, D. et al. Core-shell nanoparticles suppress metastasis and modify the tumour-
786   supportive activity of cancer-associated fibroblasts. *Journal of Nanobiotechnology.* **18**, 18 (2020).

787   31.   Sharon, Y., Alon, L., Glanz, S., Servais, C., Erez, N. Isolation of normal and cancer-
788   associated fibroblasts from fresh tissues by Fluorescence Activated Cell Sorting (FACS). *Journal of*
789   *Visualized Experiments.* (71), e4425 (2013).
790   32.   Sitia, L. et al. Selective targeting of cancer-associated fibroblasts by engineered H-ferritin
791   nanocages loaded with navitoclax. *Cells.* **10** (2), 328 (2021).
792   33.   Bellini, M. et al. Protein nanocages for self-triggered nuclear delivery of DNA-targeted
793   chemotherapeutics in cancer cells. *Journal of Controlled Release.* **196**, 184–196 (2014).
794   34.   Sahai, E. et al. A framework for advancing our understanding of cancer-associated
795   fibroblasts. *Nature Reviews Cancer.* **20**, 174–186 (2020).
796   35. Dvořánková B., Lacina L., Smetana K. Isolation of normal fibroblasts and their cancer-
797   associated counterparts (CAFs) for biomedical research.   *Methods in Molecular Biology*. **1879**,
798   393–406 (2018).
799   36. Calvo, F., Hooper, S., Sahai, E. Isolation and immortalization of fibroblasts from different
800   tumoral stages. *Bio-protocol*. **4** (7), e1097 (2014).
801   37. Sha, M. et al. Isolation of cancer-associated fibroblasts and its promotion to the progression
802   of intrahepatic cholangiocarcinoma. *Cancer Medicine*. **7** (9), 4665–4677 (2018).
803   38. Hwang, R. F. et al. Cancer-associated stromal fibroblasts promote pancreatic tumor
804   progression. *Cancer Res*earch. **68** (3), 918-926 (2008).
805   39. Zhen Z, et al. Protein nanocage mediated fibroblast-activation protein targeted
806   photoimmunotherapy to enhance cytotoxic T cell infiltration and tumor control. *Nano Letters*. **17**
807   (2), 862–869 (2017).
808   40. Ji, T. et al. Peptide assembly integration of fibroblast-targeting and cell-penetration features
809   for enhanced antitumor drug delivery. *Advances Materials*. **27** (11), 1865–1873 (2015).
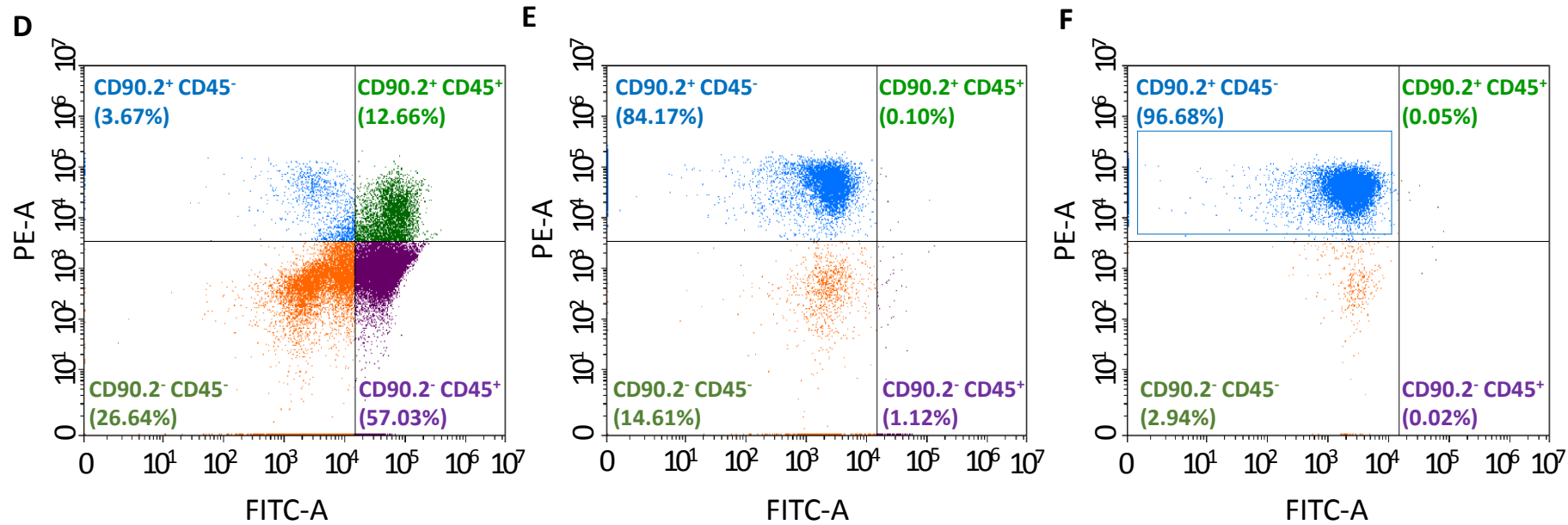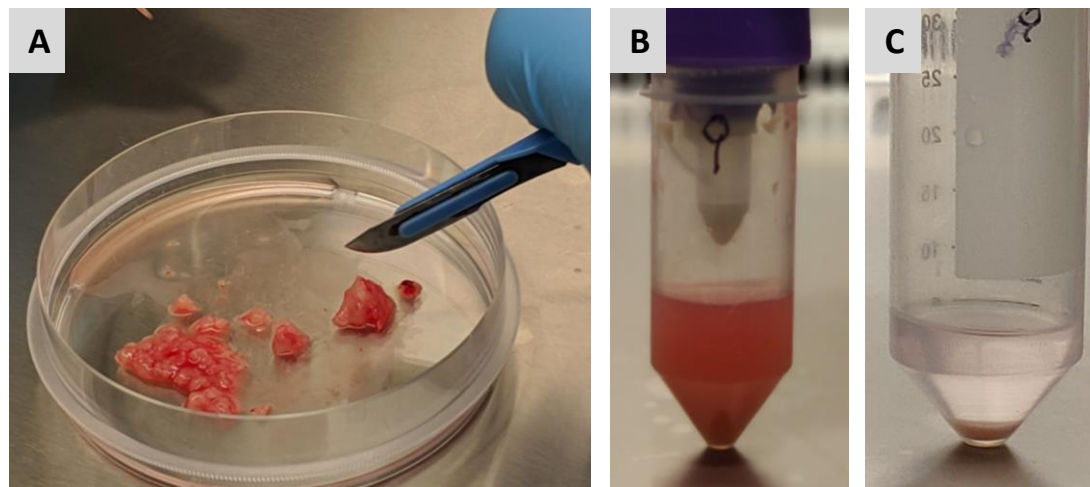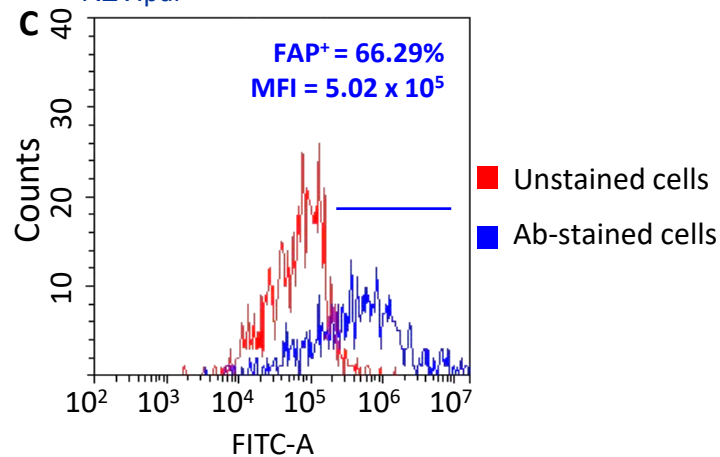810

Figure 1

A

B

C

Figure 2

Click here to access/download;Figure;Figure 2 (7).pdf ⬇

Figure 3

A

B

C

FAP$^+$ = 66.29%
MFI = 5.02 x 10^5

Counts

FITC-A

■ Unstained cells
■ Ab-stained cells

D

Figure 4

A

CD90.2⁺ CD45⁻
(84.17%)

CD90.2⁺ CD45⁺
(0.10%)

CD90.2⁻ CD45⁻
(14.61%)

CD90.2⁻ CD45⁺
(1.12%)

PE-A

FITC-A

B

C

Figure 5

A

B

Table 1
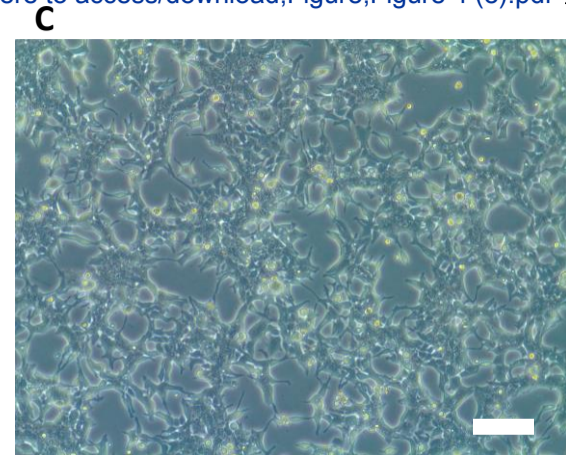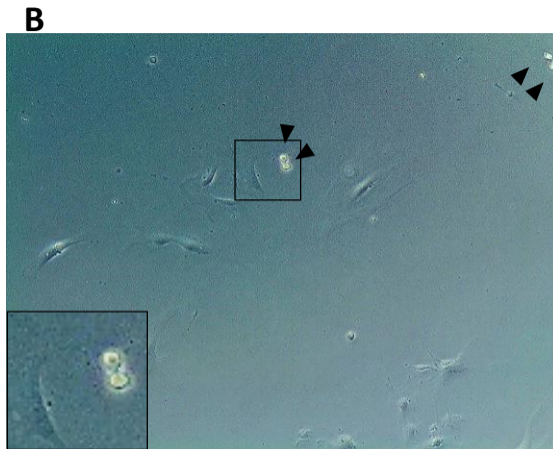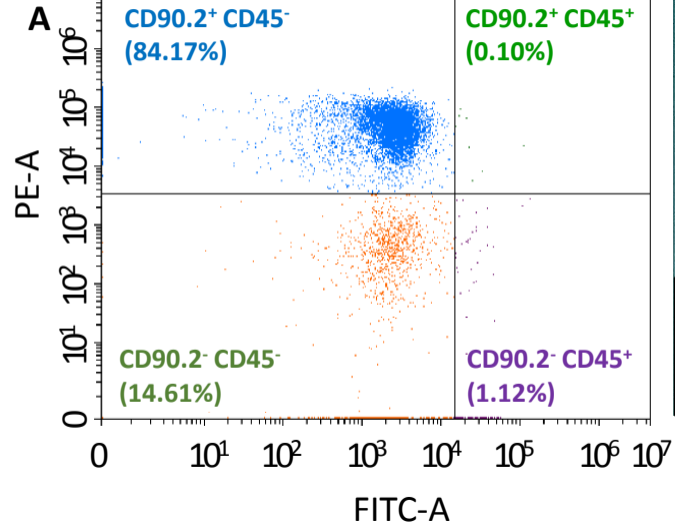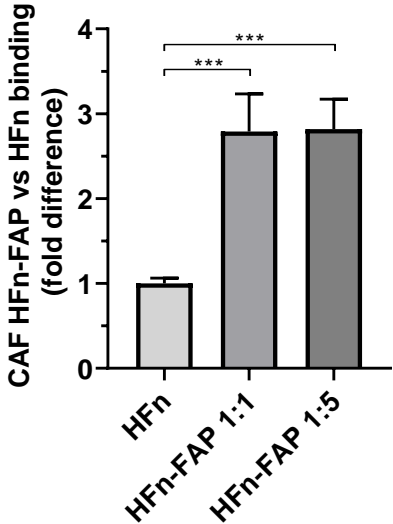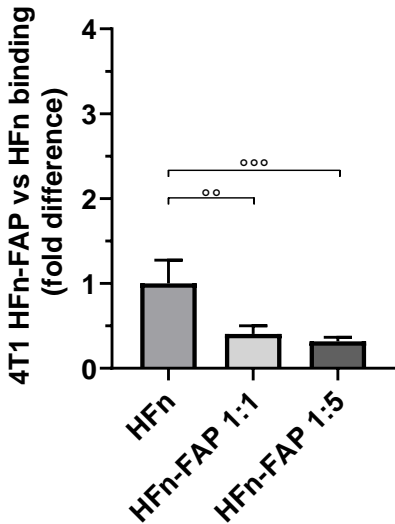
	Cell Number (average ± SD)	Extraction Yield Total (per passage)
Excised tumor (Post red blood cell removal)	$1.27 \times 10^8 \pm 9.81 \times 10^7$	100%
Excised tumor (Post dead cell removal)	$3.01 \times 10^6 \pm 9.61 \times 10^5$	2.38%
Post depletion cocktail	$1.15 \times 10^5 \pm 4.95 \times 10^4$	0.11% (3.82%)
Post enrichment	$3.00 \times 10^4 \pm 1.2 \times 10^4$	0.027% (26.09%)

Table 2

Cell Distribution (%)	CD90.2$^+$ CD45$^-$	CD90.2$^+$ CD45$^+$	CD90.2$^-$ CD45$^+$	CD90.2$^-$ CD45$^-$
Excised tumor (Post dead cell removal)	1.81 ± 0.98	10.78 ± 4.51	56.57 ± 14.05	28.20 ± 17.57
Post depletion cocktail	69.33 ± 16.75	0.14 ± 0.13	0.55 ± 0.63	39.89 ± 30.31
Post enrichment	93.14 ± 3.3	0.09 ± 0.1	0.09 ± 0.08	6.69 ± 3.4

Cell Distribution (%)	CD90.2$^+$ CD45$^-$	CD90.2$^+$ CD45$^+$	CD90.2$^-$ CD45$^+$	CD90.2$^-$ CD45$^-$
Excised tumor (Post dead cell removal)				

Table 3

Cell Distribution (%)	CD90.2$^+$ CD45$^-$	CD90.2$^+$ CD45$^+$	CD90.2$^-$ CD45$^+$	CD90.2$^-$ CD45$^-$
Post Enrichment (no pooling)	75.80 ± 2.9	1.49 ± 0.4	5.97 ± 1.5	16.75 ± 1.1

CD90.2$^+$ CD45$^-$ CD90.2$^+$ CD45$^+$ CD90.2$^-$ CD45$^+$ CD90.2$^-$ CD45$^-$

Table of Materials

Name of Material/ Equipment	Company	Catalog Number
ACK Lysing buffer	Lonza	10-548E
Alexa Fluor 488 goat anti-human antibody	Immunological Science	IS-20022
Anti-FAP Fab fragment (3F2)	Creative Biolabs	TAB-024WM-F(E)
BALB/c mice	Charles River	028BALB/C
Bovine Serum Albumin	Sigma-Aldrich	A7906
CD45 antibody	Miltenyi Biotec	130-110-796
CD90.2 antibody	Miltenyi Biotec	130-102-960
Cell strainers 70 μm	VWR	732-2758
CytoFLEX	Beckman Coulter	
Dead cell Removal Kit	Miltenyi Biotec	130-090-101
D-Luciferin	Caliper	760504
DMEM High Glucose w/o L-Glutamine w/ Sodium Pyruvate	Euroclone	ECB7501L
DMSO	Sigma-Aldrich	D2650
DPBS w/o Calcium, w/o Magnesium	Euroclone	ECB4004L
Ethylenediaminetetraacetic acid (EDTA)	Sigma-Aldrich	E9884
Fetal Bovine Serum	Euroclone	ECS0180L

Fluorescein Istothiocyanate isomer I (FITC)	Sigma-Aldrich	F7250
GentleMACS C Tubes	Miltenyi Biotec	130-096-334
GentleMACS dissociator	Miltenyi Biotec	130-093-235
Goat serum	Euroclone	ECS0200D
Ham's F12 w/o L-Glutamine	Euroclone	ECB7502L
IVIS Lumina II imaging system	Caliper Life Sciences	
LD columns	Miltenyi Biotec	130-042-901
L-Glutamine	Euroclone	ECB3000D
Light/fluorescence microscope equipped with camera	Leica Microsystems	DM IL LED Fluo/ ICC50 W CameraModule
MACS MultiStand	Miltenyi Biotec	130-042-303
MACS Separation Unit	Miltenyi Biotec	130-090-976
MACS Tissue Storage Solution	Miltenyi Biotec	130-100-008
MS columns	Miltenyi Biotec	130-042-201
Mycoplasma Removal Agent	Euroclone	ECMC210A
$NaHCO_3$	Invitrogen	A10235
Nanodrop spectrophotometer	Thermo Fisher Scientific	ND-2000C
Non essential aminoacids	Euroclone	ECB3054D
Penicillin-Streptomycin	Euroclone	ECB3001D

Recombinant Human apoferritin H-homopolymer (HFn)	Molirom	MLR-P018
RPMI 1640 w/o L-Glutamine	Euroclone	ECB9006L
Tumor-Associated Fibroblast Isolation kit	Miltenyi Biotec	130-116-474
Tumor Dissociation Kit	Miltenyi Biotec	130-096-730
Trypan blue 0.4%	Lonza	17-942E
TrypLE select	Gibco	12563-029
Trypsin-EDTA	Lonza	BE17-161E
T75 Primo TC flask	Euroclone	ET7076
Zeba Spin Desalting Columns	Thermo Fisher Scientific	89890
1.5 mL tubes	Biosigma	CL15.002.0500
15 mL tubes	Euroclone	ET5015B
4T1-luc2	Caliper	
50 mL tubes	Euroclone	ET5050B

Comments/Description

Store at +15° to +30 °C.

Protect from light.

7 weeks old female mice
Store at 2-8 °C.

FITC-conjugated fluorescent antibody; clone REA 737; Store protected from light at 2–8 °C.
PE-conjugated fluorescent antibody; clone 30-H12; Store protected from light at 2–8 °C.

laser configuration B4-R2-V0
contains 10 mL of Dead Cell Removal MicroBeads; 25 mL of 20× Binding Buffer Stock Solution. Store protected from light at 2–8 °C.

reagent for *in vivo* imaging

Warm at 37 °C in a water bath before use.

Keep at room temperature.

Before use, heat at 56 °C for 30 min to kill all the complement proteins.

Store protected from light at 2–8 °C.

They are used in combination with the gentleMACS Dissociator.
Two samples can be processed in parallel. Special protocols have been
developed for various tissues.

Warm at 37 °C in a water bath before use.

This imaging system is easy to use for both fluorescent and bioluminescent imaging in
vivo. Equipped with a Living Image Software for analysis
Composed of ferromagnetic spheres, designed for stringent depletion of
unwanted cells. Position the required number of columns on the magnetic

200 mM stock

inverted microscope for live cells with camera

Position the magnet on appropriate stand before use.

Composed of ferromagnetic spheres, designed for positive selection of cells.
Position the required number of columns on the magnetic Separation Unit
Dilute in culture medium 1:100.

Warm at 37 °C in a water bath before use.

Contains 1 mL of Non-Tumor-Associated Fibroblast Depletion Cocktail, mouse; 1 mL of CD90.2 (Tumor-Associated Fibroblast) MicroBeads,mouse. Store protected from light at 2-8 °C.

Contains lyophilized enzymes (D, R, A) and buffer A; reconstitute enzymes according to the manufacturer's instructions, aliquot and store at - 20 °C.
dilute 1:1 with a sample of cell suspension before counting the cells
use at room temperature
Warm at 37 °C in a water bath before use

7K MWCO, 2 mL

Mouse mammary gland cancer cell line stably transfected with firefly luciferase gene

Istituti Clinici Scientifici Maugeri

March 29ᵗʰ, 2021

To the Editor of *Journal of Visualized Experiments*

Dear Editor,

I propose, for your kind attention, the revised version of the manuscript entitled "Isolation of primary cancer-associated fibroblasts from a syngeneic murine breast cancer: a model to study targeted nanoparticles" by Mart Truffi, Leopoldo Sitia, Marta Sevieri, Arianna Bonizzi, Maria Antonietta Rizzuto, Serena Mazzucchelli and Fabio Corsi, to be considered for publication in *Journal of Visualized Experiments*.

Point-by point reply to reviewers and editor

Editorial comments:

Editorial Changes

Changes to be made by the Author(s):

1. Please take this opportunity to thoroughly proofread the manuscript to ensure that there are no spelling or grammar issues.

We thank for this suggestion. The manuscript has been proofread for grammar and spelling errors.

2. Please define all abbreviations before use.

Thank you for these corrections. The paper has been amended.

3. For in-text citations, use "…formation5,6,8." instead of "…formation.5,6,8"

The citations are now included in the article as requested.

4. Maintain a 0-inch left indent throughout the text and indicate new paragraphs using single-line spacing. Justify all text.

The paper has been amended as requested.

5. Please remove the formatting from the tables.

ICS Maugeri SpA SB è certificata secondo la UNI EN ISO 9001:2015 da Bureau Veritas Italia SpA

Istituti Clinici Scientifici Maugeri Spa - Società Benefit IRCCS
via Salvatore Maugeri, 4 - 27100 Pavia | Codice fiscale e Partita Iva: 02631650187 | cod. univoco fatt. elettronica: MZO2A0U
Iscrizione Rea: PV – 289202 | tel. 0382 592504 | email: info@icsmaugeri.it

The tables have been amended; bold fonts and margins have been removed.

6. Please add details about the age, sex, breed of the mice used.

We thank for this suggestion. Required information has been included in the revised manuscript.

7. Line 146: Please clarify "..1/2 mice..".

The paper has been amended as requested.

8. Line 254: Could you add more details about column preparation?

We thank for this suggestion. For columns preparation it is sufficient that a magnetic stand is placed under the hood and that ferromagnetic separation columns (one column for up to 107 cells) are hung up on it with the tip pointing down. Then 0.5 mL of cold 1× Binding Buffer is placed on the column to equilibrate them. When the solution has passed through by gravity, the columns are ready for incubation with the bead/cell suspension for magnetic separation. The revised version of the manuscript now contains more details.

9. Line 560: Please check the value in Table 2.

We thank for this comment. We have checked values in Table 2, which are correct. Accordingly, we have decided to amend the text as follows:

"The depletion beads cocktail efficiently removes CD45+ cells (accounting for 67.35% and 0.69% of total cells pre- and post-depletion, respectively, Table 2)".

10. Add a single space between the quantity and its unit. E.g. use "2 mm" instead of "2mm". Please use decimal points instead of "," (line 506).

Thank you for these corrections. The paper has been amended.

11. JoVE cannot publish manuscripts containing commercial language. This includes trademark symbols (™), registered symbols (®), and company names before an instrument or reagent. Please remove all commercial language from your manuscript and use generic terms instead. All commercial products should be sufficiently referenced in the Table of Materials. E.g. IVIS Lumina II, gentleMACS, etc.

The paper has been amended as requested.

12. Please ensure that the references appear as the following: [Lastname, F.I., LastName, F.I., LastName, F.I. Article Title. Source. Volume (Issue), FirstPage – LastPage (YEAR).] For more than 6 authors, list only the first author then et al. Do not abbreviate journal names. Please include volume and issue numbers for all references.

The references have been formatted to better fit the journal requests

13. Please sort the Materials Table alphabetically by the name of the material.

 The Materials Table is now alphabetically sorted

Reviewer #1:

Manuscript Summary:

Isolation of primary cancer-associated fibroblasts from a syngeneic murine breast cancer: a model to study targeted nanoparticles

This manuscript reports a method outlining the isolation of primary cancer-associated fibroblasts from a murine breast cancer cell line to enable ex vivo testing of nanoparticles. The present work is informative and well presented, it is recommended that the paper be accepted with minor revisions.

We thank the Reviewer for the overall positive judgement of our manuscript. A point-by-point response to the raised comments is available below.

The suggestions to improve the manuscript are presented below.

1. Introduction, page 1, Line 71. Replace "throughout" with "thorough".

Thank you for this correction. The paper has been amended.

2. Protocol, page 7, section 3.2.4. Replace "trice" with "thrice"

Thank you for this correction. The paper has been amended.

3. Representative results, page 12, line 554. "…dead cells is found..." replace "is" with "are"

Thank you for this suggestion. In the examined sentence the term "is" was referred to "a high percentage" instead of "dead cells"; therefore, the singular third person was used. We hope that the Reviewer agree with us to let it as "is"

ICS Maugeri SpA SB è certificata secondo la UNI EN ISO 9001:2015 da Bureau Veritas Italia SpA

Istituti Clinici Scientifici Maugeri Spa - Società Benefit IRCCS
via Salvatore Maugeri, 4 - 27100 Pavia | Codice fiscale e Partita Iva: 02631650187 | cod. univoco fatt. elettronica: MZO2A0U
Iscrizione Rea: PV – 289202 | tel. 0382 592504 | email: info@icsmaugeri.it

4. Figure 3. Cell Morphology. These images could benefit with altering the contrast to better show the shape/outline of the cells.

Thank you for this suggestion. The images have been adjusted for contrast.

5. Figure 3. Cell Morphology. The cells imaged do have fibroblastic morphology, but perhaps the readers would benefit here from an additional image of the native 4T1 for comparison to the isolated fibroblasts.

According to the Reviewer suggestion, a bright-field image of 4T1 tumor cells has been added as Figure 3 d.

6. Discussion, page 15, line 680. "…for long time." Insert "a" to make "for a long time".

The sentence has been amended as requested.

Reviewer #2:

Manuscript Summary:

The authors have elaborately described the methods for isolating cancer-associated fibroblasts from the murine breast cancer model. The study further employs the isolated CAFs to study the targeting capability of nanoparticles targeting the tumor microenvironment.

Minor Concerns:

1. The authors have described the methods very well which increases the reproducibility of the protocol. Furthermore, the authors have provided a list of chemicals, company names and catalogue numbers at the end which makes it easy to reproduce. However, the authors might need to check with the journal if their way of presenting the methods matches their manuscript requirements.

We thank the Reviewer for the overall positive comment to our manuscript. We have carefully followed the manuscript template from JoVE and we believe that the methods section now fits the journal requirements.

2. The authors have not mentioned the methods of statistical analysis used in this paper.

Thanks to the reviewer for pointing out this missing point. As suggested, in the revised version of the manuscript we included in the Protocol Section a new paragraph dedicated to the statistical analysis (6.3).

ICS Maugeri SpA SB è certificata secondo la UNI EN ISO 9001:2015 da Bureau Veritas Italia SpA

Istituti Clinici Scientifici Maugeri Spa - Società Benefit IRCCS
via Salvatore Maugeri, 4 - 27100 Pavia | Codice fiscale e Partita Iva: 02631650187 | cod. univoco fatt. elettronica: MZO2A0U
Iscrizione Rea: PV – 289202 | tel. 0382 592504 | email: info@icsmaugeri.it

3. I was wondering if the authors could organise the results in subsections. This will make it easy for the reader to focus on all points.

Many thanks for this precious suggestion. We revised the results section by creating three subsections entitled: In vivo model set-up for optimal CAF isolation;

Optimization of CAF isolation procedure, culture and characterization;

Use of isolated cells to evaluate CAF targeting potential of engineered nanodrugs.

4. I am not sure if the authors mention how many animals were used and how many times each experiment was performed in the text.

We thank the reviewer for this comment. We included the total number of animals used for the experiments in a new paragraph (6.1) of the Protocol Section.

5. I was wondering if the authors have performed any statistical tests for the flow cytometry.

Thanks for raising the topic. We did perform an analysis of the statistical differences among the cell populations found in the four quadrants after the three steps of cell isolation (reported here below). However, we did not include it in the main text, as this was mainly oriented to prove the efficacy of the protocol, while we did not want to make a comparison between ours and other methods.

6. It is not clear if the authors used any protein markers for the characterisation of CAFs.

We thank the reviewer for pointing out such an important point. Here, we first stained isolated cells with anti CD45 and CD90.2 antibodies. Then, we confirmed CAF characteristics by evaluating Fibroblast Activation Protein (FAP) expression by cytofluorimetry on isolated cells, as FAP is the most widely used and reliable marker for CAF characterization. In another study that we recently published, we further characterized isolated CAFs by evaluating FAP and α Smooth Muscle Actin (α SMA) expression by Western Blot, in comparison with 4T1 cells (Reference 32: Sitia L. et al. Cells. 2021 Feb 5;10(2):328), thus confirming the success of the isolation procedure.

7. The authors have not mentioned the number of times an experiment was performed for testing of Fbn on isolated cancer-associated fibroblasts.

Thanks for the comment. We added a paragraph in the protocol section (6.2) with the requested information.

8. In the discussion section, the authors need to mention more about nanomedicine and CAFs. Furthermore, if this method or any similar technique has been used for any other type of cancer in research.

We thank the reviewer for this suggestion that will improve our manuscript. We added two new paragraphs in the discussion, mentioning more methods of CAF isolation and some classes of nanomedicines that are being developed to specifically target CAFs.

9. Line 44 "reprogramming"

Thank you for this correction. The paper has been amended.

We have addressed to all issues raised by reviewers and we believe that this paper is now suitable for publication in *Journal of Visualized Experiments*.

All authors approve the submission of the present manuscript, which has been submitted exclusively to *Journal of Visualized Experiments.* None of the materials contained in this manuscript has been published or is under consideration elsewhere. There is no conflict of interest for this work.

Sincerely yours,
Fabio Corsi

Prof. Fabio Corsi
Head of Breast Unit
Surgery Department
Istituti Clinici Scientifici Maugeri IRCCS
Via Maugeri 4, 27100, Pavia - Italia
phone: +39 0382592272 email: fabio.corsi@icsmaugeri.it
Associate Professor of General Surgery
Department of Biomedical and Clinical Sciences L. Sacco

University of Milan
via G.B. Grassi, 74-20157 Milan (Italy)
phone: +39 0250319850-19858 email: fabio.corsi@unimi.it